Rance, M., Sorensen, O. W., Bodenhausen, G., Wagner, G., & Ernst, R. R. (1983) *Biochem. Biophys. Res. Commun. 69*, 979-987.
Richardson, J. S., Getzoff, E. D., & Richardson, D. C. (1978) *Proc. Natl. Acad. Sci. U.S.A. 75*, 2574-2578.
Schiffer, M., Ainsworth, C., Xu, Z. B., Carperos, W., Olsen, K., Solomon, A., Stevens, F. J., & Chang, C. H. (1989) *Biochemistry 28*, 4066-4072.
Schildbach, J. F., Panka, D. J., Parks, D. R., Jager, G. C., Herzenberg, L. A., Mudgett-Hunter, M., Haber, E., & Margolies, M. N. (1991) *J. Biol. Chem. 266*, 4640-4647.
Shaka, A. J., Keeler, J., Frenkiel, T., & Freeman, R. (1983) *J. Magn. Reson. 52*, 335.
States, D. J., Haberkorn, R. A., & Ruben, D. J. (1982) *J. Magn. Reson. 48*, 286-292.
Stevens, F. J., Westholm, F. A., Solomon, A., & Schiffer, M. (1980) *Proc. Natl. Acad. Sci. U.S.A. 77*, 1144-1148.
Stevens, F. J., Chang, C. H., & Schiffer, M. (1988) *Proc. Natl. Acad. Sci. U.S.A. 85*, 6895-6899.
Stevens, F. J., Solomon, A., & Schiffer, M. (1991) *Biochemistry 30*, 6803-6805.
Takahashi, H., Odaka, A., Kawaminami, S., Matsunga, C., Kato, K., Shimada, I., & Arata, Y. (1991) *Biochemistry 30*, 6611-6619.
Ward, E. S., Guessow, D., Griffiths, A. D., Jones, P. T., & Winter, G. (1989) *Nature 341*, 544-546.
Wright, P. E., Dyson, H. J., Lerner, R. A., Riechmann, L., & Tsang, P. (1990) *Biochem. Pharmacol. 40*, 83-88.
Wüthrich, K. (1986) *NMR of Proteins and Nucleic Acids*, John Wiley & Sons, New York.

Glycosylinositol Phospholipid Anchors of the Scrapie and Cellular Prion Proteins Contain Sialic Acid†

Neil Stahl,‡ Michael A. Baldwin,‡ Rolf Hecker,‡ Keh-Ming Pan,‡ Alma L. Burlingame,§ and Stanley B. Prusiner*,‡,∥

Departments of Neurology, Pharmaceutical Chemistry, and Biochemistry and Biophysics, University of California, San Francisco, California 94143

Received October 3, 1991; Revised Manuscript Received January 31, 1992

ABSTRACT: The only identified component of the scrapie prion is PrP^{Sc}, a glycosylinositol phospholipid (GPI)-linked protein that is derived from the cellular isoform (PrP^{C}) by an as yet unknown posttranslational event. Analysis of the PrP^{Sc} GPI has revealed six different glycoforms, three of which are unprecedented. Two of the glycoforms contain *N*-acetylneuraminic acid, which has not been previously reported as a component of any GPI. The largest form of the GPI is proposed to have a glycan core consisting of Manα-Manα-Man-(NeuAc-Gal-GalNAc-)Man-GlcN-Ino. Identical PrP^{Sc} GPI structures were found for two distinct isolates or "strains" of prions which specify different incubation times, neuropathology, and PrP^{Sc} distribution in brains of Syrian hamsters. Limited analysis of the PrP^{C} GPI reveals that it also has sialylated glycoforms, arguing that the presence of this monosaccharide does not distinguish PrP^{C} from PrP^{Sc}.

Recent research has substantiated the unusual molecular nature of the pathogens causing scrapie and other transmissible neurodegenerative disorders, but their exact structure and replicative mechanism remain enigmatic (Prusiner, 1991). These pathogens were named prions (Prusiner, 1982) because diverse experimental approaches have consistently failed to reveal the participation of a nucleic acid in their transmission to inoculated recipients (Alper et al., 1967; Bellinger-Kawahara et al., 1987, 1988; Duguid et al., 1988; Oesch et al., 1988; Meyer et al., 1991). In contrast, numerous results establish that a host-encoded protein designated PrP^{Sc} [1] is a component of the scrapie prion (Bolton et al., 1982; McKinley et al., 1983; Gabizon et al., 1988; Scott et al., 1989; Prusiner et al., 1990; Hsiao et al., 1989, 1990). PrP^{Sc} is a disease-specific isoform of a normal cellular protein of unknown function denoted PrP^{C} (Oesch et al., 1985; Basler et al., 1986). In addition to scrapie, prions containing PrP are implicated in the transmissible human neurodegenerative diseases kuru, Creutzfeldt-Jakob disease (CJD), and Gerstmann-Sträussler-Scheinker disease (GSS) (Gajdusek, 1977; Masters et al., 1981; Prusiner, 1987). Several varieties of CJD and GSS are unique in that the disease occurs in families with an autosomal dominant pattern

† This work was supported by grants from the NIH (NS14069, AG02132, NS22786, and AG08967) and the American Health Assistance Foundation as well as by gifts from the Sherman Fairchild Foundation and National Medical Enterprises. R.H. was supported by a fellowship from the European Molecular Biology Organization. The Bio-organic, Biomedical Mass Spectrometry Resource (A. L. Burlingame, Director) was supported by National Institutes of Health National Center for Research Resources Grant RR01614 and by National Science Foundation Biological Instrumentation Program Grant DIR8700766.

* To whom correspondence should be addressed at the Department of Neurology, HSE-781, University of California, San Francisco, CA 94143-0518.
‡ Department of Neurology.
§ Department of Pharmaceutical Chemistry.
∥ Department of Biochemistry and Biophysics.

[1] Abbreviations: PrP^{Sc}, scrapie isoform of the prion protein; PrP^{C}, cellular isoform of the prion protein; PrP 27-30, N-terminally truncated form derived from PrP^{Sc} by limited proteolysis; GPI, glycosylinositol phospholipid; PIPLC, phosphatidylinositol-specific phospholipase C; K12-GPI, C-terminal GPI-linked peptide purified after digestion of PrP with endoproteinase Lys-C and PIPLC; LSIMS, liquid secondary ion mass spectrometry; ESP, electrospray mass spectrometry; CE, capillary electrophoresis; HPAE, high-pH anion exchange; NANA, *N*-acetylneuraminic acid; GlcN, glucosamine; GalNAc, *N*-acetylgalactosamine; Ino, inositol; Man, mannose; Gal, galactose.

0006-2960/92/0431-5043$03.00/0

of inheritance, yet brain tissue from the afflicted individuals contains transmissible prions. All of the inherited human prion diseases are associated with mutations in the PrP gene (Hsiao & Prusiner, 1990; Doh-ura et al., 1989; Owen et al., 1989; Goldgaber et al., 1989; Goldfarb et al., 1990; Hsiao et al., 1989, 1991a,b). The newest prion disease is bovine spongiform encephalopathy (BSE or "mad cow disease"), which was apparently transferred inadvertantly in offal contaminated with sheep scrapie prions and has infected >50 000 British cows (Wilesmith et al., 1988).

A crucial goal toward understanding scrapie and prions is to decipher the difference between PrP^C and PrP^{Sc} (Stahl & Prusiner, 1991). The two isoforms have different physical properties: PrP^C is soluble in detergents and is sensitive to digestion with proteases (Oesch et al., 1985; Meyer et al., 1986), while PrP^{Sc} aggregates in the presence of detergent and gives rise to a resistant core called PrP 27–30 through loss of the N-terminus upon limited proteolysis (McKinley et al., 1991). Experiments in scrapie-infected neuroblastoma cells reveal that PrP^{Sc} is formed with a half-time of 2 h from a protease-sensitive precursor by a posttranslational event (Borchelt et al., 1990). This posttranslational event could be a chemical modification, a conformational change, or tight association with other cellular components. Although numerous posttranslational chemical modifications of PrP^{Sc} have been found (Stahl & Prusiner, 1991; Bolton et al., 1985; Stahl et al., 1987, 1990a; Hope et al., 1988; Turk et al., 1988; Endo et al., 1989), they all appear to be present in PrP^C as well. While only detailed comparison of the chemical structure of PrP^{Sc} and PrP^C will reveal any differences, the structures known for the PrP^{Sc} modifications do not appear unique, and there is no obvious candidate that would give altered physical properties and make PrP^{Sc} a prion component.

The glycosylinositol phospholipid (GPI) was discovered as we began to catalog the chemical modifications found on PrP 27–30 (Stahl et al., 1987). Both PrP^C and PrP^{Sc} are modified by GPI anchors, but it is unknown whether their exact structures differ and could thus play a role in the pathogenesis or transmission of scrapie. Although the GPI diradylglycerol from both PrP isoforms is cleaved by phosphatidylinositol-specific phospholipase C (PIPLC) after the proteins are denatured (Stahl et al., 1990b), only PrP^C, and not PrP^{Sc}, is released from cellular membranes upon incubation with the enzyme (Stahl et al., 1990b; Caughey et al., 1990). We have therefore undertaken structural analysis of the PrP 27–30 GPI; purified PrP^C is not yet available in sufficient amounts to permit complete characterization. Previous analysis of the Syrian hamster PrP 27–30 GPI has indicated that it is attached at Ser_{231} (Stahl et al., 1990a). Permethylation and tandem mass spectrometry revealed the composition and branching pattern of the glycan core (Baldwin et al., 1990a), which showed some structures similar to those reported for rat brain Thy-1 (Homans et al., 1988), and an additional form with a hexose attached to the *N*-acetylhexosamine. In this paper, we report the existence of PrP 27–30 GPI species that contain neuraminidase-sensitive sialic acid. Furthermore, we show that the PrP^C GPI contains similar sialylated species.

Another fascinating aspect of scrapie is the existence of distinct prion isolates or "strains" that differ in their properties with respect to incubation time, neuropathology, and distribution of PrP^{Sc} in the brain (Bruce & Dickinson, 1987; Carp & Callahan, 1991; Fraser & Dickinson, 1968; Hecker et al., 1992). While strains of viruses or viroids have genomes with different nucleic acid sequences that confer strain-specific properties, the apparent lack of demonstrable nucleic acid in the prion would require a novel mechanism to produce heritable characteristics. Although many investigators have argued that the occurrence of distinct prion isolates demands the existence of a prion-specific nucleic acid, there is no theoretical reason why such characteristics could not be heritably encoded in other chemical structures or in protein conformation. We present evidence here indicating that the structure of the PrP 27–30 GPI is identical for two distinct prion isolates. These findings argue that the properties of prion isolates are not determined by the PrP^{Sc} GPI structure.

Experimental Procedures

Endoproteinase Lys-C (sequencing grade), *Arthrobacter ureafaciens* neuraminidase, jack bean α-mannosidase, and digoxigenin-linked lectins were purchased from Boehringer Mannheim. PIPLC either was a gift from Martin Low or was purified by an identical procedure. Purification of Syrian hamster PrP 27–30, as well as the procedure for solubilization, digestion with endoproteinase Lys-C and PIPLC, and purification of the GPI-linked C-terminal peptide (K12-GPI) by reverse-phase HPLC, has been described previously (Stahl et al., 1990a). The prion isolate used for most of the studies reported here caused neurological disease ~75 days after intracerebral inoculation of Syrian hamsters; it is designated Sc237 (Scott et al., 1989) and is similar to the isolate labeled 263K (Kimberlin & Walker, 1978). The data shown in Figures 1 and 5B used PrP 27–30 purified by ultrafiltration from hamsters infected with a prion strain called 139H (Hecker et al., 1992); indistinguishable spectra are obtained when PrP 27–30 purified from hamsters infected with the standard Sc237 strain is used.

Partial Purification of PrP^C. PrP^C was purified by a new procedure (K.-M. Pan, N. Stahl, and S. B. Prusiner, unpublished results). Normal hamster brains (25 g) were homogenized in 9 volumes (v/w) of 0.25 M sucrose, 1 mM PMSF, 10 mM sodium phosphate (pH 7.0), and 0.15 M NaCl with a Polytron for 40 s with a 15-s break every 10 s. After centrifugation at 3000*g* for 30 min, the pellet was discarded, and the supernatant was centrifuged again for 1 h at 100000*g*. The resultant pellet was solubilized in 50 mL of PBS (10 mM sodium phosphate, pH 7.0, and 0.15 M NaCl) containing 8% ZW 3-12 (Calbiochem, La Jolla, CA). The suspension was stirred at 4 °C for 1 h and then centrifuged at 100000*g* for another hour. The final supernatant was applied onto a chelating Sepharose Fast Flow (5 × 10 cm) (Pharmacia, Sweden; Sulkowski, 1989), which was charged with Cu^{2+} and prepared according to the procedure of Andersson et al. (1987). The column was washed in succession with 10 mM imidazole and 0.2% ZW 3-12 in PBS, and 0.1 M sodium acetate (pH 4.0) and 0.5 M NaCl. Finally, PrP^C was eluted with 50 mM EDTA, 10 mM sodium phosphate (pH 7.0), and 0.2 M NaCl. The PrP-containing EDTA eluant was collected, 36 g of urea was added per 100 mL, and the pH was adjusted to 6.0 with 2 N HCl. The mixture was loaded onto a cation exchanger of sulfonic type (Bio-Rad, 1.5 × 8 cm), which was equilibrated in 5 M urea, 0.1% ZW 3-12, 10 mM sodium phosphate, pH 6.0, and 0.2 M NaCl (buffer A). After the column was washed with buffer A, PrP^C was eluted by buffer A containing 0.5 M NaCl. PrP^C-enriched fractions were pooled and stored at −20 °C until use.

α-Mannosidase Digest of GPI Glycans. An HPLC fraction containing K12-GPI was treated with aqueous HF and repurified to give GPI glycan as described (Baldwin et al., 1990b). A fraction containing 500 pmol was brought to pH ~5 with 60 mM sodium acetate buffer and digested overnight at room temperature with 0.25 unit of jack bean α-manno-

sidase in a final volume of 80 μL. Alternatively, an HPLC fraction containing 925 pmol of K12-GPI was dried in a SpeedVac, then reconstituted with 77 mM sodium acetate buffer at pH ~5, and digested overnight at room temperature with 0.25 unit of α-mannosidase in a final volume of 65 μL.

GPI Permethylation, Liquid Secondary Ion Mass Spectrometry (LSIMS), and Tandem Mass Spectrometry. Incubation of K12-GPI in aqueous HF, permethylation, and mass spectrometric analysis have been described in detail (Baldwin et al., 1990b). To improve the recovery of the sialylated GPI species, the supernatant fraction was removed from the remaining sodium hydroxide following permethylation, and 10 μL of acetic acid was added before drying and extraction of the sample as previously described.

Electrospray Mass Spectrometry. A VG Bio-Q mass spectrometer was used (VG BioTech Ltd., Altrincham, U.K.). The sample buffer was 1:1 H_2O/CH_3CN containing 1% acetic acid and 2 pmol/μL gramicidin S, pumped by an ABI Model 130 pump at 4 μL/min into the atmospheric pressure ionization chamber from a nebulizer consisting of a needle held at 4 kV with a coaxial nitrogen supply. Samples were injected into the liquid flow via a Rheodyne microinjector fitted with a 10-μL loop. The mass spectrometer was set for repetitive 10-s scans, and its performance was optimized by monitoring the doubly protonated molecular ion of gramicidin S at m/z 571.7. The mass scale was calibrated by injecting 100 pmol of myoglobin (molecular mass 16250.6 Da) and monitoring the multiply charged peaks in the range 600–1400 m/z. Multiple spectra were acquired over a period of 3 min and averaged under computer control. The data were smoothed using Savitsky–Golay algorithms. In electrospray mass spectrometry (ESP), molecular ions having n excess protons and thus n positive charges are observed at m/z values corresponding to $(M_r + n)/n$. By fitting different possible integer values of n to this equation, series of ions can be identified originating from a common molecular mass M_r.

Dionex High-pH Anion-Exchange (HPAE) Chromatography. An aliquot of an HPLC fraction containing approximately 1 nmol of K12-GPI was digested with 1 μg/mL Pronase (Boehringer Mannheim) in 50 mM Tris (pH 8.45) at 37 °C for 1 h. Half of this sample was brought to pH ~4 with acetic acid and incubated with 0.05 unit of neuraminidase at 37 °C for 2 h. Both fractions were analyzed by Dionex HPAE chromatography on a CarboPac PA100 (25 × 0.4 cm) column with pulsed amperometric detection. The mobile phase was 100 mM NaOH with a linear gradient of sodium acetate from 50 mM at 1 min to 170 mM at 60 min. Samples for monosaccharide analysis containing 555 pmol of K12-GPI were dried in microfuge tubes, treated with or without incubation in 50% aqueous HF for 40 h at 4 °C, and then hydrolyzed at 100 °C for 2 h in either 4 M TFA (neutral sugar analysis) or 6 M HCl (amino sugar analysis). Monosaccharides were separated on the CarboPac PA100 column isocratically at 16 mM sodium hydroxide, and quantitated by peak area relative to 500-pmol monosaccharide standards. Analysis of sialic acid released by either neuraminidase digestion (0.05 unit, 2 h) or mild acid hydrolysis (100 mM HCl at 80 °C for 1 h) was carried out isocratically in 100 mM sodium hydroxide and 50 mM sodium acetate.

Capillary Electrophoresis. Samples were analyzed by the absorbance at 200 nm on a Beckman P/ACE fitted with an uncoated capillary. Separations were carried out toward the cathode in 100 mM phosphate buffer (pH 2.5) at an operating voltage of 20 kV at 25 °C. Samples of K12-GPI were brought to pH ~4 with sodium acetate buffer, incubated at room temperature with or without addition of neuraminidase (3 units of 5-μL total volume for 2 h), and then injected pneumatically into the instrument.

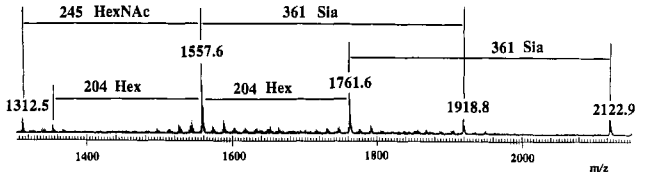

FIGURE 1: LSIMS analysis of permethylated GPI glycans. The difference between the various peaks with indicated masses corresponds to the following permethylated saccharides: sialic acid (Sia), hexose (Hex), or *N*-acetylhexosamine (HexNAc). A detailed description of the three low-mass peaks can be found in Baldwin et al. (1990a,b).

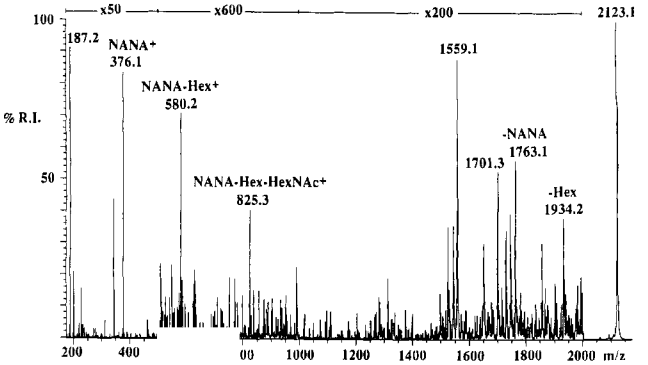

FIGURE 2: Tande permethylated GPI glycan containing sialic acid. The spectrum snows the daughter ions resulting from collision-induced dissociation of the permethylated glycan of mass 2123.1. The ions marked–Hex and –NANA correspond to species that have lost a hexose or sialic acid from the parent ion. The peaks marked $NANA^+$, $NANA\text{-}Hex^+$, and $NANA\text{-}Hex\text{-}HexNAc^+$ indicate the compositions of the relevant ions. The scales at the top show multiplication factors used in plotting various portions of the spectrum.

Gel Electrophoresis. SDS–PAGE was performed according to Laemmli (1970) and two-dimensional gels by the method described previously (Oesch et al., 1990). Electrotransfer and blotting were carried out as described (Stahl et al., 1987); incubation and staining with the digoxigenin-linked lectins were executed as suggested by the manufacturer.

RESULTS

Mass Spectrometry of Permethylated GPI Glycans. In the initial GPI structural characterization, we had purified the GPI-linked C-terminal peptide (called K12-GPI) from PrP 27–30 by reverse-phase HPLC following digestion with endoproteinase Lys-C and PIPLC (Stahl et al., 1990a). Incubation of this peptide at 4 °C in 50% aqueous HF allowed recovery of both the peptide and GPI glycan for subsequent analysis (Stahl et al., 1990a). Permethylation of the glycan increased the hydrophobicity for LSIMS and gave easily characterized fragmentation upon high-performance tandem mass spectrometry that allowed assignment of the order and branching for three to four forms of the GPI glycan (Baldwin et al., 1990a). During the course of that analysis, we became aware of two other glycoforms with m/z = 1918.8 and 2122.9 that were observed in approximately two of six experiments. The masses of these two glycoforms differed from lower mass species by the addition of *N*-acetylneuraminic acid (Figure 1). A modification of the method used for permethylation resulted in reproducible observation of the sialylated forms (see Experimental Procedures), although it is likely that further refinement of this procedure might give improved recoveries of all the GPI glycan species.

Tandem mass spectrometry of the sialylated glycan with m/z = 2122.9 was performed to reveal the attachment point

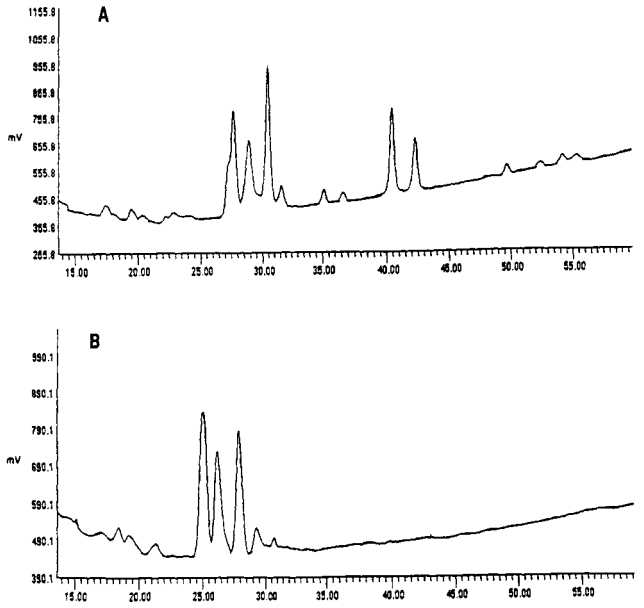

FIGURE 3: Dionex HPAE chromatography of PrP 27–30 GPI. Panel A shows the elution of the GPI, while panel B shows the chromatogram observed when the sample is predigested with neuraminidase. The horizontal axis is time in minutes, and the vertical axis represents signal output in millivolts from the pulsed amperometric detector.

of the sialic acid (Figure 2). The pattern of fragmentation observed was more complex than the simple spectra obtained for the unsialylated glycoforms, which showed numerous informative daughter ions that corresponded to $^{1,5}X$ fragmentation cleavages across the sugar rings with charge retention on the aglycon fragment (Baldwin et al., 1990a). Several ions in the high-mass region can be explained by loss of either a hexose or a sialic acid from the parent ion as indicated in Figure 2, but the identity of every fragment is not obvious and would require discussion more appropriate for another venue. However, the low-mass region of this spectrum shows prominent "B" or oxonium ions corresponding to fragments composed of $NANA^+$, $NANA\text{-}Hex^+$, and $NANA\text{-}Hex\text{-}HexNAc^+$ (Figure 2). This array of fragments indicates that the sialic acid is attached to the hexose found on the HexNAc branch of the glycan.

High-pH Anion-Exchange Chromatography. Further evidence for the presence of sialylated GPI species was obtained by HPAE chromatography on a Dionex system. Following digestion of K12-GPI with Pronase, which leaves only a single serine residue attached to the GPI ethanolamine as shown by amino acid analysis (data not shown), HPAE chromatography separated the GPI into a series of five major peaks (Figure 3A). Neuraminidase pretreatment of the sample eliminated the peaks eluting at 40.5 and 42 min, and shifted their migration times to match those of the earlier peaks (Figure 3B). A control experiment with Pronase treatment of an HPLC fraction containing a nonglycosylated peptide from a neighboring HPLC fraction showed no corresponding peaks in its chromatogram (data not shown).

Dionex HPAE was used to examine the carbohydrate composition of the PrP 27–30 GPI following hydrolysis with either 4 M trifluoroacetic acid or 6 M HCl. The neutral sugar analysis after TFA hydrolysis revealed the presence of mannose and galactose, while both glucosamine and galactosamine were observed upon analysis of the amino sugars (Table I). The amount of mannose observed was near 1, while a value of 4 was expected on the basis of analogy to the structure for rat brain Thy-1 (Homans et al., 1988). However, preincubation in aqueous HF, which removes phosphates from the glycan,

Table I: Carbohydrate Composition of K12-GPI and the GPI Glycan[a]

	K12-GPI (−aqueous HF)	GPI glycan (+aqueous HF)
mannose	1.1	5.4
galactose	0.6	0.9
glucosamine	0.3	0.3
galactosamine	1.2	1.1
N-acetylneuraminic acid	0.25	nd[b]

[a] Monosaccharides were quantitated by Dionex HPAE chromatography, and the values were normalized by the amount of sample used as measured by quantitative amino acid analysis (Stahl et al., 1990a). The values for the GPI glycan were measured after removal of phosphoethanolamines by incubation in aqueous HF. Neutral sugar analysis followed hydrolysis with TFA, while amino sugars were quantitated after hydrolysis with HCl as described under Experimental Procedures. The value for *N*-acetylneuraminic acid was measured following either mild acid hydrolysis or release with neuraminidase. [b] Not determined.

increased the amount of mannose observed to >5, while the amount of galactose remained relatively constant (Table I). The value for mannose is close to one of 4 predicted from the other structural data, and argues that the phosphoethanolamines are linked to mannose residues as proposed for Thy-1 (Homans et al., 1988). The amount of glucosamine recovered is only 30% of the expected value assuming one residue per GPI, as indicated by the mass spectra. It is likely that this value is artificially low, perhaps from an inhibiting effect of the protonated 2′-ammonium substituent on the rate of glycosidic bond cleavage through an acid-catalyzed carbocation mechanism. Dionex HPAE chromatography under other conditions confirmed that a species comigrating with authentic *N*-acetylneuraminic acid was released from the PrP 27–30 GPI at a mole fraction of ~0.25 by either neuraminidase or mild acid hydrolysis. Myoinositol was identified in previous experiments involving prolonged acid hydrolysis and GCMS analysis of the residue following trimethylsilylation (Stahl et al., 1987, 1990c).

The carbohydrate composition revealed the presence of one galactose residue in the PrP 27–30 GPI; no other GPI from a mammalian source has been shown to contain this monosaccharide. It is compatible, however, with the observation of an NANA-Hex-HexNAc branch of the GPI as indicated by the high-energy collision-induced dissociation mass spectrum in Figure 2. This trisaccharide is reminiscent of the common *O*-linked trisaccharide NANAα(2–3)Galβ(1–3)-GalNAc which is attached to serine (Beyer et al., 1981), as well as structures found on some gangliosides (Fiezi, 1985).

Lectin Binding to the PrP 27–30 GPI. Although lectins are widely used to characterize both O-linked and N-linked oligosaccharides, we are not aware of any published reports of lectin binding to GPI anchors. The K12-GPI peptide derived from endoproteinase Lys-C digest of purified PrP 27–30 can be separated by SDS–PAGE and efficiently electrotransferred to nitrocellulose if the lipid is not removed by PIPLC (Stahl et al., 1990a). The position of this GPI-linked peptide on the blot is revealed by an antibody (called α-P3) which is specific for the 11 amino acid peptide bound to the GPI (Figure 4, lanes 1 and 2). Lectin binding to the GPI was assessed by incubation of the blot with digoxigenin-tagged lectins, followed by detection with alkaline phosphatase-conjugated anti-digoxigenin. Ricin, which binds terminal β-galactosyl residues, binds weakly to a band comigrating with K12-GPI (Figure 4, lane 3). Removal of sialic acid with neuraminidase gives a small but detectable increase in the staining intensity (Figure 4, lane 4), implying that the interaction with ricin is specific.

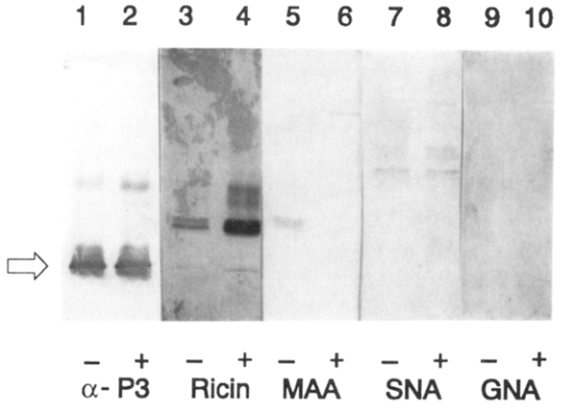

FIGURE 4: Lectin binding to the PrP 27–30 GPI. Purified PrP 27–30 was digested with endoproteinase Lys-C, then subjected to SDS–PAGE in a 12.5% acrylamide gel, and electrotransferred to nitrocellulose. The even-numbered lanes (indicated by +) were preincubated with neuraminidase before electrophoresis. The blot was cut into strips and incubated with the antibody or lectin indicated in the figure. See the text for a description of the specificities of antibody and lectins used. The arrow indicates the migration position of the C-terminal GPI-linked peptide K12-GPI.

This result suggests that the sialic acid is linked to the galactose as NANA-Gal-GalNAc, since some of the galactose residues would only become terminal after removal of the sialic acid. The ricin staining observed higher on the blot corresponds to the 75 amino acid K8 peptide which contains a heterogeneous, sialylated N-linked sugar chain (Endo et al., 1989).

The results with other lectins were disappointing; none tested gave any detectable staining of the GPI. Neither MAA (*Maackia amurensis* agglutinin), which is specific for sialic acid linked $\alpha(2-3)$ to galactose, nor SNA (*Sambucus nigris* agglutinin), which recognizes sialic acid linked $\alpha(2-6)$ to galactose, binds to the K12-GPI band (Figure 4, lanes 5–8). MAA, however, does bind to the K8 oligosaccharide (Figure 4, lane 5) in a neuraminidase-sensitive fashion (Figure 4, lane 6). Although the K8 and K12-GPI peptides are presumably present on the blot in equimolar amounts, it is possible that the lack of staining results from insufficient sample loaded as only 25% of the GPI contains sialic acid, while each K8 oligosaccharide may have three to four sialic acid residues (Endo et al., 1989). The lectin GNA (*Galanthus nibalis* agglutinin) recognizes terminal mannose that is $\alpha(1-3)$, $\alpha(1-6)$, or $\alpha(1-2)$ linked to mannose, yet does not bind the PrP 27–30 GPI (Figure 4, lane 9). Although we demonstrate below that the GPI terminal mannose is α-linked to another mannose (see Figure 7), probably in an $\alpha(1-2)$ configuration as in rat brain Thy-1, it is possible that the presence of the ethanolamine phosphate on the penultimate mannose interferes with GNA binding. This hypothesis predicts that GNA should bind the GPI glycan after removal of the phosphates with aqueous HF.

Electrospray Mass Spectrometry of K12-GPI. Although the methods outlined above revealed a great deal about the structure of the PrP 27–30 GPI, we were concerned that the incubation with aqueous HF and subsequent permethylation in NaOH/DMSO could possibly remove a labile group, giving a misleading view of the actual GPI structure. We therefore pursued analysis of intact K12-GPI by ESP, which is capable of measuring the mass of very large molecules with relatively high accuracy through the formation of multiply protonated ions. To simplify the electrospray mass spectra, we first separated the sialylated from unsialylated K12-GPI species by reverse-phase HPLC in 10 mM sodium acetate at pH 7.0 (Figure 5A). This method gave two resolved sets of peaks, the earlier of which eluting near 34 min contained the sialylated forms. ESP was carried out following repurification of these two fractions by RP-HPLC in a standard TFA buffer to remove the sodium acetate. The earlier eluting acidic fraction contains two main components with masses of 3124.6 and 3285.8 (Figure 5B), while the second fraction contain three components with masses of 2671.0, 2832.5, and 2994.4 (Figure 5C). It should be noted that the spectra shown here have been transformed for clarity by an algorithm that displays the data on a scale of molecular weight, not on a scale of m/z with ions containing +2, +3, or +4 charges that were actually observed.

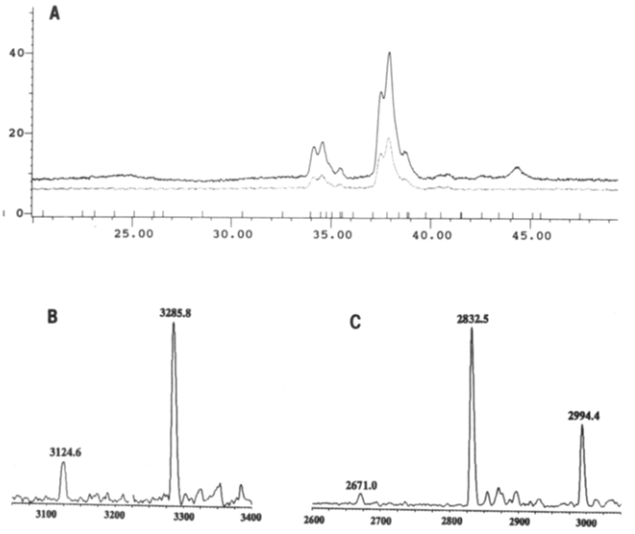

FIGURE 5: Separation and electrospray mass spectrometry of various K12-GPI glycoforms. (A) K12-GPI purified by reverse-phase HPLC in buffers containing TFA was re-injected on a C-18 column and eluted with buffers containing 10 mM sodium acetate (pH 7) and an acetonitrile gradient of 0.5% per minute following a 10-min isocratic wash at 0% buffer B. The solid line indicates the absorbance observed at 214 nm, while the dotted line shows the absorbance observed at 280 nm. The absorbance at 280 nm is plotted on a scale that is 5-fold more sensitive than that at 214 nm. The electrospray mass spectrum of the fraction eluting at 34 min is shown in panel B, while panel C shows the spectrum of the fraction eluting near 38 min. The electrospray data consisting of peaks with different numbers of charges have been transformed to an axis that simply represents molecular weight. The peak intensities in panels B and C were scaled independently and are not quantitative.

These masses can be accounted for by the structures shown in Figure 6. These display the glycan core structures that were observed by LSIMS attached to the C-terminal peptide at Ser_{231} through a phosphoethanolamine moiety. Additionally, the measured mass requires the presence of a second phosphoethanolamine, as suggested previously by amino acid analysis (Stahl et al., 1987), and a phosphate monoester attached at the inositol that remained from the PIPLC digest. The masses calculated for these structures are indicated in Figure 6, and match the observed masses within 1 mass unit. The calculated values are based on the averaged atomic weights for the elements since the quadrupole-based electrospray mass spectrometer is unable to resolve the natural-abundance isotopic profile.

α-Mannosidase Digests of the PrP 27–30 GPI. The GPI glycan from rat brain Thy-1 (Homans et al., 1988) contained three α-mannose groups that could be removed with jack bean α-mannosidase. We therefore carried out a similar experiment with the PrP 27–30 GPI glycan following removal of phosphate groups with aqueous HF. The products of the α-mannosidase digest were then analyzed by LSIMS following permethylation (Figure 7A). Three new species were observed with masses of 1149.4, 1353.5, and 1714.9, concomitant with the loss of nearly all the species observed in Figure 1. The new species

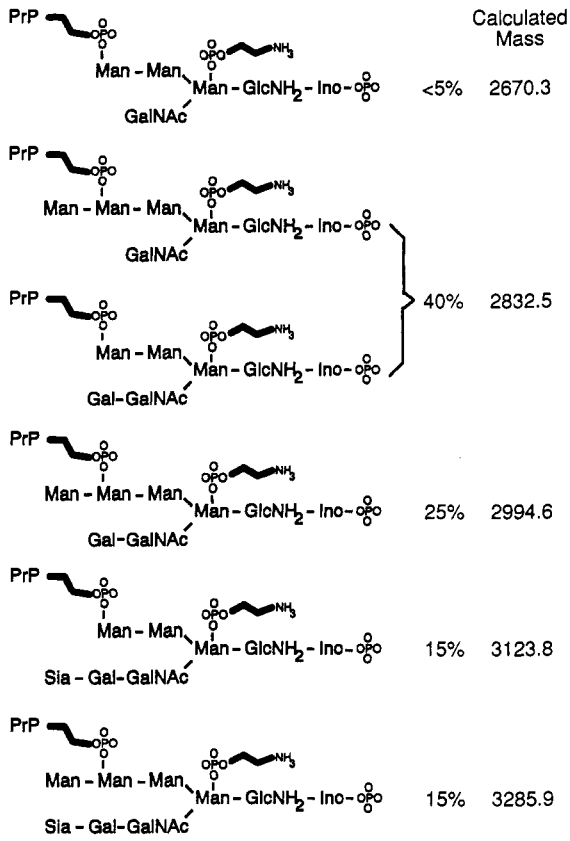

FIGURE 6: Proposed structures for six glycoforms of the PrP 27–30 GPI. See the Discussion for details as to which features are based on analogy to other anchors. The percentages indicate an estimate of the aproximate relative abundance of each glycoform, based on the data in Figures 1, 3, 5, and 9, as well as Table I. The calculated masses are based on the average molecular weight of each element in the GPI, and include the mass of the K12 peptide (which accounts for 1312.5 mass units of the total) to allow comparison to the experimental data in Figure 5.

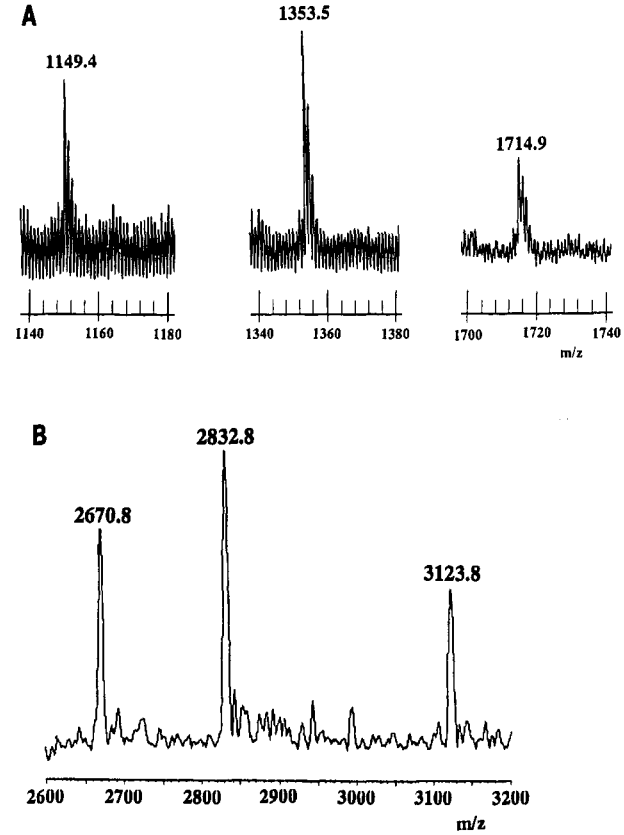

FIGURE 7: Analysis of the GPI glycan and GPI anchor after α-mannosidase digestion. Either the GPI glycan (isolated after removal of phosphoethanolamines by aqueous HF; panel A) or the intact K12-GPI (panel B) was digested with jack bean α-mannosidase as described under Experimental Procedures and then analyzed by mass spectrometry to decipher how many mannose residues were removed. In panel A, the glycan was permethylated and analyzed by LSIMS, while in panel B K12-GPI was analyzed by electrospray mass spectrometry. The data in panel A should be compared to those in Figure 1, while the data in panel B should be compared to Figure 5B,C.

correspond to the loss of either one or two hexose groups from the original array of species to give a common core with heterogeneity only on the *N*-acetylhexosamine branch. Thus, these data indicate that up to two hexose groups were removed from the GPI glycan, not three as expected from the results reported for Thy-1. It is presently unknown whether this result implies that an α-mannose is not present in this position in the PrP 27–30 GPI glycan or that insufficient α-mannosidase was used in the digest. α-Mannosidase was used at 100 units/mL in the Thy-1 experiments (Homans et al., 1988), while the PrP 27–30 GPI glycan was incubated with only 3 units/mL.

A similar α-mannosidase digest of the intact GPI from Thy-1 resulted in removal of only one mannose group, indicative of the presence of a phosphate group attached to the penultimate mannose (Homans et al., 1988). A similar experiment involving α-mannosidase digestion of intact K12-GPI gave three peaks with masses of 2670.8, 2832.8, and 3123.8 upon subsequent analysis by ESP (Figure 7B). The loss of the molecules with masses 3285.8 and 2994.4, and the lack of appearance of molecules with masses lower than 2671, indicates that a single mannose was removed. Thus, removal of the second mannose is blocked by a moiety that is sensitive to aqueous HF, consistent with attachment of a phosphoethanolamine at the penultimate mannose as in Thy-1.

Analysis of the PrP^C GPI for Sialic Acid. Since the presence of sialic acid on a GPI has not been previously reported, it was conceivable that the occurrence of this monosaccharide on the PrP^{Sc} GPI was the critical difference responsible for the distinct physical properties of PrP^C and PrP^{Sc}. Because purification of substantial amounts of PrP^C has not yet been achieved, application of the methods used for analyzing the PrP 27–30 GPI was not possible. We therefore examined the PrP^C GPI for the presence of sialic acid by two different methods applicable to partially purified preparations. The first method consisted of performing two-dimensional gel electrophoresis on endoproteinase Lys-C digested samples, followed by specific detection of K12-GPI peptide on immunoblots with the α-P3 antibody. Analysis of the PrP 27–30 GPI indicated two sets of GPI species with different isoelectric points (Figure 8A), the most acidic of which could be eliminated by pretreatment with neuraminidase (not shown). Similar analysis of a hamster brain fraction enriched for PrP^C revealed a similar staining pattern with a faint but detectable fraction of acidic K12-GPI species corresponding to the sialylated GPI glycoforms as indicated by the arrow in Figure 8B.

More compelling evidence for the presence of a sialic acid on the PrP^C GPI was obtained by capillary electrophoresis (CE), which separates molecules on the basis of their charge to size ratio. CE of the HPLC-purified C-terminal peptide from PrP 27–30 (K12-GPI) at pH 2.5 in 100 mM sodium phosphate buffer indicated the presence of at least two groups of peaks by absorbance detection at 200 nm (Figure 9A). K12-GPI elutes later than most other peptides because the three phosphate groups retain a significant amount of negative charge at pH 2.5 relative to most amino acid side chains,

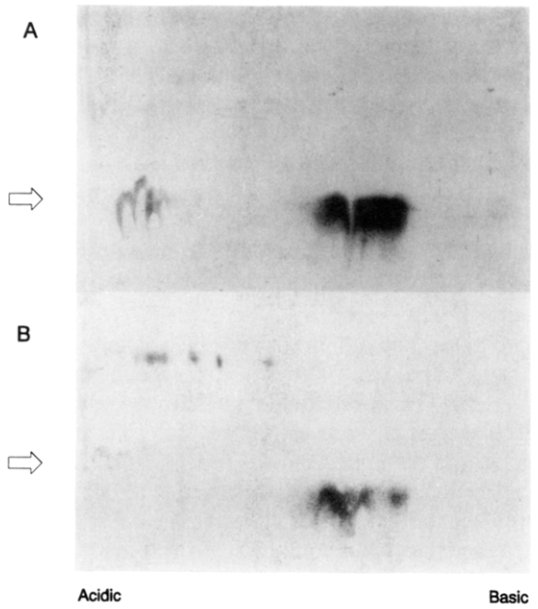

FIGURE 8: Two-dimensional gel analysis of K12-GPI to detect sialylated GPI glycoforms. Samples consisting of purified PrP 27–30 (A) or partially purified PrP^C (B) were digested with endoproteinase Lys-C and then subjected to isoelectric focusing in the first dimension using ampholines with a pH range of 3–10, followed by SDS–PAGE (12.5% acrylamide) in the second dimension. The peptides were electrotransferred to nitrocellulose, and the K12-GPI was detected with the α-P3 antibody which is specific for the C-terminal peptide that is attached to the GPI. The arrows indicate the positions of the sialylated forms which have a more acidic p*I*.

causing slower migration toward the cathode. Pretreatment of the GPI with neuraminidase resulted in the disappearance of the late-eluting species, consistent with the presence of neuraminidase-sensitive sialic acid (Figure 9F). A commensurate increase in the area under the nonsialylated peaks was always observed upon neuraminidase digestion. Partially purified fractions containing hamster PrP^C were digested by endoproteinase Lys-C and PIPLC, and separated by reverse-phase HPLC. PrP^C was not the major protein in this preparation; therefore, the HPLC fractions eluting around the retention time observed for PrP 27–30 K12-GPI were reduced in volume and systematically examined for the presence of K12-GPI by CE. One fraction revealed a series of peaks by capillary electrophoresis with a remarkably similar pattern to that observed for PrP 27–30, including those migrating at 43 min that contain sialic acid as indicated by the arrows in Figure 9B. The migration times of peptides can vary somewhat between runs, but co-injection of the PrP^C and PrP 27–30 samples revealed that the peaks exactly comigrated (not shown). Although the fraction containing PrP^C is not pure, all of the putative K12-GPI peaks disappeared after treatment with aqueous HF (Figure 9C), in a manner similar to that observed for purified K12-GPI derived from PrP 27–30 (Figure 9D). Preincubation of the sample with neuraminidase results in disappearance of the peaks corresponding to the sialylated forms of the K12-GPI (Figure 9E), providing strong evidence for the presence of *N*-acetylneuraminic acid on the PrP^C GPI.

All of the ESP analysis of the PrP 27–30 GPI clearly revealed masses corresponding to an inositol phosphate monoester, while the product of the reaction catalyzed by the bacterial PIPLC is thought to be a mixture of inositol 1-phosphate and inositol cyclic 1,2-phosphate (Taguchi et al., 1980). Conversion of the cyclic product to a phosphate monoester is accelerated under acidic conditions and has been described previously (Ferguson et al., 1985). CE analysis of freshly isolated K12-GPI revealed shoulders eluting after the

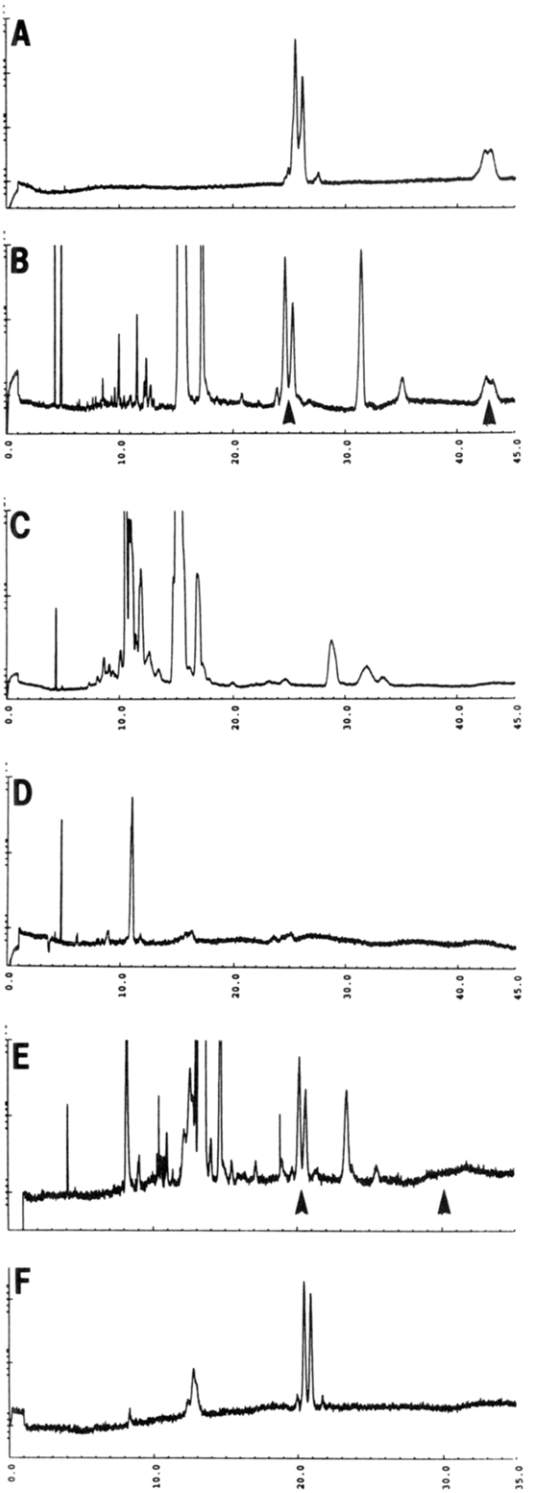

FIGURE 9: Capillary electrophoresis of HPLC fractions containing K12-GPI from PrP 27–30 and PrP^C. Each panel shows the electrophoretogram of HPLC-purified fractions following endoproteinase Lys-C and PIPLC digests of purified PrP 27–30 (panels A, D, and F) or partially purified PrP^C (panels B, C, and E). The samples in panels C and D were incubated with 50% aqueous HF for 36 h before analysis, while the samples in panels E and F were digested with neuraminidase before electrophoresis. The migration times of peaks can vary somewhat between runs; co-injection of the samples shown in panels A and B verified comigration of the K12-GPI derived from PrP 27–30 and PrP^C (not shown). The migration times in panels E and F were carried out with a different batch of buffer and varied substantially from that observed in the other panels. The arrows in panels B and E indicate the elution positions of K12-GPI glycoforms; the position of the sialylated species in panel E was confirmed in a control experiment carried out the same day (not shown). The peak appearing at approximately 13 min in panels E and F was derived from the neuraminidase added to the sample.

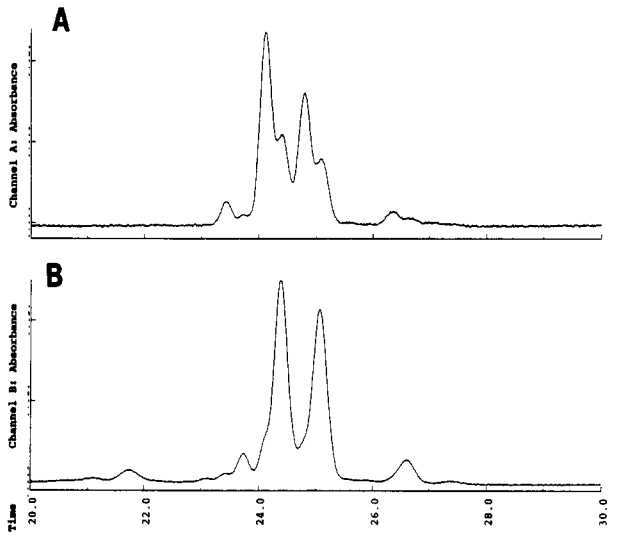

FIGURE 10: Capillary electrophoresis of K12-GPI ± boiling. Freshly purified K12-GPI derived from PrP 27–30 after PIPLC digestion is shown in panel A. Boiling the sample gives the electrophoretogram in panel B. The change in behavior is attributed to the opening of the cyclic phosphate left on inositol by the PIPLC digest as discussed in the text.

main peaks migrating between 24 and 25 min (Figure 10A). Samples stored at 4 °C in HPLC buffer showed a gradual increase in the size of the shoulders with concomitant loss of the earlier peaks over a period of weeks (e.g., Figure 9A). Briefly boiling the HPLC fraction (which contains ~0.06% TFA) before analysis shifts the elution time of the main peaks to match those of the shoulders, consistent with the opening of a cyclic phosphate ring (Figure 10B). Furthermore, the process of drying and resuspension carried out before analysis by ESP gave electrophoretograms identical to that seen after boiling as in Figure 10B. We also observed that this brief boiling, but not drying and resuspension of the peptide, resulted in complete loss of the sialic acid from the glycan (not shown).

Analysis of the GPI from a Second Prion Isolate. We examined the structure of the GPI from a second prion isolate designated 139H (Kimberlin et al., 1987) to uncover any differences that might play a role in specifying the characteristics of distinct prion isolates. All of the data revealed GPI structures that were indistinguishable from those described for the first isolates, Sc237 prions. The mass spectra shown in Figures 1 and 5B were actually acquired from the GPI derived from 139H prions; similar experiments with Sc237 gave equivalent results. Capillary electrophoresis of K12-GPI from the two prion isolates also gave identical electrophoretograms. Although we have not yet compared the carbohydrate composition and linkage of the GPI from both isolates, there is no indication of any prion isolate-specific structures.

Discussion

The process by which PrP^{Sc} is formed posttranslationally from a protease-sensitive precursor remains uncertain. The elucidation of the chemical structure of PrP^{Sc} has thus far revealed that N-linked glycosylation (Haraguchi et al., 1989) and the GPI anchor (Stahl et al., 1987) constitute the bulk of the covalent posttranslational modifications to both the cellular and abnormal isoforms of PrP (Stahl & Prusiner, 1991). Partial structures of the N-linked carbohydrate are known for PrP^{Sc}, and while extremely heterogeneous, there is no obvious way in which they could contribute to the altered physical properties exhibited by PrP^{Sc} (Endo et al., 1989). Furthermore, ablation of the N-linked sites in PrP by site-directed mutagenesis does not eliminate the acquisition of protease resistance upon expression of the protein in scrapie-infected neuroblastoma cells (Taraboulos et al., 1990). Although it is not yet known for certain whether the protease-resistant PrP without N-linked sites is still associated with scrapie infectivity, there are no reports of samples containing protease-resistant PrP^{Sc} in the absence of scrapie infectivity. We examined the structure of the GPI anchor to determine whether a scrapie-specific structural feature existed that might play a role in giving PrP^{Sc} its abnormal properties.

Structural Heterogeneity of the PrP^{Sc} GPI. The data presented in this and a previous paper (Baldwin et al., 1990a) permit us to propose the six structures for the PrP^{Sc} GPI shown in Figure 6. The approximate relative percentages of the various glycoforms were estimated from the spectra and chromatograms obtained from LSIMS, ESP, HPLC, CE, and HPAE, the last being both with and without hydrolysis. Although the assignment of glucosamine and not galactosamine as the unacetylated amino sugar was made by analogy to other GPI structures, substantive evidence shows the order and branching of the sugar units by mass, the position of the two α-mannose groups, and the lack of acetylation on the inositol-linked hexosamine. Furthermore, the ricin binding data suggest that the galactose residue is β-linked. The α-mannosidase digest revealed the location of one phosphoethanolamine on the penultimate mannose. The attachment point of the second phosphoethanolamine residue was predicted on that determined for rat brain Thy-1, although the data in Table I assert that the phosphates are indeed linked to mannose in the PrP 27–30 GPI. We originally predicted a stoichiometry of 2.8 ethanolamines on the GPI anchor, but it is likely that this value is erroneous: it was obtained after adjustment of the observed value of 1.8 by a hydrolysis loss factor determined for an ethanolamine standard (Stahl et al., 1987). The mass obtained by electrospray mass spectrometry clearly indicates the lack of a third ethanolamine, and our mass spectrometric analysis of the remainder of PrP 27–30 (N. Stahl, M. A. Baldwin, D. Teplow, L. Hood, B. Gibson, A. L. Burlingame, and S. B. Prusiner, unpublished results) excludes the possibility of any non-GPI ethanolamine (Dever et al., 1989).

Sialylated GPI Anchors Are Unprecedented. A novel feature of the structures from PrP is the presence of sialic acid on ~30% of the GPI anchors. This is not a scrapie-specific feature, however, since Figures 8 and 9 clearly demonstrate the presence of sialylated GPI glycoforms on PrP^{C}. Since the N-linked oligosaccharide chains of PrP^{C} are unnecessary for conversion of the protein to PrP^{Sc} (Taraboulos et al., 1990), the GPI provides the last known posttranslational modification that might harbor differences between PrP^{C} and PrP^{Sc}. We have not yet completed assignment of the anomeric configuration and linkage positions of the glycosidic bonds, nor determination of the second lipid moiety which is attached to the PrP 27–30 GPI along with stearic acid (Stahl et al., 1987). Although these detailed comparisons with the PrP^{C} GPI remain to be finished, the identical behavior of the PrP^{C} and PrP 27–30 K12-GPI by both HPLC and capillary electrophoresis suggests that their anchor structures are likely to be similar in size, charge, and point of attachment. The heterogeneity in sialylation at the GPI would contribute to the diversity of isoelectric points observed for both PrP^{Sc} and PrP^{C} on two-dimensional gels after removal of the N-linked carbohydrate by peptide *N*-glycosidase F (Haraguchi et al., 1989).

Comparison of Distinct Prion Isolates. It is also evident that the presence of the sialic acid in the PrP^{Sc} GPI is not responsible for the isolate-specific characteristics of 139H

prions. Analysis of the 139H-derived GPI revealed that it is identical in mass, retention in reverse-phase HPLC and capillary electrophoresis, and level of heterogeneity. It has not been excluded that the GPI anchor from the two distinct prion isolates could differ by glycosidic linkage or the type of lipid attached. We are continuing the detailed comparison of PrP^{Sc} from both the 139H and Sc237 strains to identify chemical differences that could account for their distinct scrapie incubation times, neuropathology, and distribution of PrP^{Sc} in the brain (Hecker et al., 1992). If no chemical differences are found, then either prions possess as yet unidentified non-PrP components or PrP^{Sc} exists in different conformations which determine the properties of each distinct isolate (Prusiner, 1991).

Sialic Acid and Metabolic Regulation. Although there is as yet no information regarding the purpose, if any, of the sialic acid attached to the prion protein GPI, there is a growing appreciation of the important regulatory roles served by sialic acid on glycoproteins and glycolipids (Rademacher et al., 1988). Examples include lymphocyte migration and homing (Samlowski et al., 1984; Rosen et al., 1989), regulation of cell adhesion by polysialic acid on NCAM (Acheson et al., 1991), and modulation by gangliosides of basic fibroblast growth factor efficacy (De Cristan et al., 1990), CD4 function (Offner et al., 1987), neurite outgrowth in neuroblastoma cells (Tsuji et al., 1983), PDGF receptor phosphorylation (Bremer et al., 1984), and insulin receptor tyrosine kinase activity (Nojiri et al., 1991). The identification of sialic acid on a GPI anchor now presents the possibility for participation of GPI anchors in similar functions. There is also the opportunity for distinctive specificities if protein-derived GPI moieties function as growth factor second messengers (Low & Saltiel, 1988; Romero et al., 1988).

While the observation of a sialic acid residue on the PrP GPI is unprecedented, this may simply reflect the fact that only a few GPI structures are known. It is unlikely that similar glycoforms were missed in the analysis of rat brain Thy-1 GPI since the presence of the sialic acid and hexose attached to the GalNAc should have been detected by the methods used. The proposed structure of the GPI trisaccharide branch containing the sialic acid is NANA-Gal-GalNAc, which is similar to the common trisaccharide NANAα(2–3)Galβ(1–3)GalNAc that is attached to serine hydroxyl groups in some proteins (Beyer et al., 1981), as well as the SSEA-4 ganglioside antigen (Feizi, 1985). It is not yet known whether the PrP GPI has similar linkage positions or anomeric configurations, and whether previously identified glycosyltransferases are responsible for creating this structure. The observation that the lectin MAA, which is specific for α(2–3)-linked sialic acid, failed to bind to the PrP GPI on blots may have resulted from loading insufficient sample. The fact that ricin binds to a band comigrating with the PrP 27–30 K12-GPI is consistent with a β-linkage for galactose. The detectable increase in ricin binding observed after pretreatment with neuraminidase would be expected on the basis of the diversity of glycoforms observed by the analytical analysis.

Sugars of the PrP^{Sc} GPI Glycans. The PrP 27–30 GPI structures all contain a common core glycan also found in the six other GPI moieties that have been analyzed in detail (Schmitz et al., 1987; Ferguson et al., 1988; Homans et al., 1988; Roberts et al., 1988; Mayor et al., 1990; Schneider et al., 1990). This core consists of three mannose residues, glucosamine, and inositol. This matches the structure of the putative GPI precursor characterized for trypanosomes (Mayor et al., 1990); the structure of mammalian GPI precursors is not known (Singh et al., 1991). All of the carbohydrate heterogeneity would be consistent with secondary modifications of a common core matching the trypanosome GPI precursor. Evidence consistent with secondary modification of the GPI after its attachment to the protein has been observed (Bangs et al., 1988). GPI anchors are almost certainly attached to proteins in the endoplasmic reticulum (Bangs et al., 1985), and further monosaccharide addition would be expected to occur as the protein traversed the Golgi and trans-Golgi network on its way to the cell surface. The addition of *N*-acetylneuraminic acid to the PrP^{Sc} GPI probably occurs in the Golgi as this is the purported localization of known sialyltransferases (Paulson & Colley, 1989), and sialylated proteins are apparently not found in earlier regions of the protein export pathway (Tartakoff & Vassalli, 1983). However, it should be noted that a cell surface trans-sialidase has recently been identified in *Trypanosoma cruzi* (Zingales et al., 1987; Schenkman et al., 1991).

The observation of at least five GPI glycoforms by Dionex HPAE chromatography confirms that the heterogeneity observed by both LSIMS of the permethylated glycan and electrospray mass spectrometry of K12-GPI is not artifactual and reflects naturally occurring GPI species. This degree of glycan heterogeneity is somewhat greater than that reported for other mammalian GPI anchors (Homans et al., 1988; Roberts et al., 1988). One additional minor glycoform lacking the HexNAc branch was observed only after aqueous HF treatment. This is probably an artifact associated with partial lability of this bond in aqueous HF, and was also observed for the Thy-1 GPI (Homans et al., 1988).

Mass Spectrometry and GPI Structure Determination. The results described here demonstrate that ESP is useful for the characterization of GPI anchors. In conjunction with the LSIMS and MS/MS analysis of the permethylated GPI glycan released by aqueous HF, ESP confirmed the general structure, disclosed the number of phosphoethanolamines, and provided reassurance as to the actual level of heterogeneity of the sample. We expect that the presence of the C-terminal peptide is probably required for obtaining mass information in the positive ion mode with ~200 pmol of sample as in Figure 5, but we have not investigated this point. We have also not attempted ESP in the negative ion mode, which may prove effective as the molecule contains several phosphate ions.

Conclusions. Our findings substantially narrow the search for chemical modifications that might feature in posttranslational conversion of PrP^{C} to PrP^{Sc}. Our observations on two distinct prion isolates strengthen the conclusion that PrP GPI anchors are unlikely to be responsible for either the novel features of PrP^{Sc} or the specific biological properties of prion isolates. Prion proteins are the first molecules described with sialic acid residues attached to GPI glycans; in addition, earlier studies showed that sialic acids are attached to some of the N-linked complex-type oligosaccharides of PrP^{Sc} (Endo et al., 1989). Thus, some of the size and charge heterogeneity exhibited by PrP^{Sc} (Bolton et al., 1985) is due to sialic acids. Whether the number and position of sialic acids attached to PrP glycans influence the fate of the cellular or scrapie PrP isoforms remains to be established.

ACKNOWLEDGMENTS

We thank Fisons Instruments for loan of the BioQ mass spectrometer. We are grateful to Mike Ferguson, Tom Rademacher, and Raymond Dwek for their earlier participation in the structural analysis as well as Brad Gibson for his interest and advice. We are also indebted to Dr. E. Sulkowski for suggesting IMAC purification of PrP. We further thank Lorri

Reinders, Dave Maltby, Sherman Jew, Indrani Mitra, and Darlene Groth for their technical expertise.

References

Acheson, A., Sunshine, J. L., & Rutishauser, U. (1991) *J. Cell Biol. 114*, 143–153.

Alper, T., Cramp, W. A., Haig, D. A., & Clarke, M. C. (1967) *Nature (London) 214*, 764–766.

Andersson, L., Sulkowski, E., & Porath, J. (1987) *Cancer Res. 47*, 3624–3626.

Baldwin, M. A., Stahl, N., Reinders, L. G., Gibson, B. W., Prusiner, S. B., & Burlingame, A. L. (1990a) *Anal. Biochem. 191*, 174–182.

Baldwin, M. A., Stahl, N., Burlingame, A. L., & Prusiner, S. B. (1990b) *Methods: Compan. Methods Enzymol. 1*, 306–314.

Bangs, J. D., Hereld, D., Krakow, J. L., Hart, G. W., & Englund, P. T. (1985) *Proc. Natl. Acad. Sci. U.S.A. 82*, 3207–3211.

Bangs, J. D., Doering, T. L., Englund, P. T., & Hart, G. W. (1988) *J. Biol. Chem. 263*, 17697–17705.

Basler, K., Oesch, B., Scott, M., Westaway, D., Wälchli, M., Groth, D. F., McKinley, M. P., Prusiner, S. B., & Weissmann, C. (1986) *Cell 46*, 417–428.

Bellinger-Kawahara, C., Diener, T. O., McKinley, M. P., Groth, D. F., Smith, D. R., & Prusiner, S. B. (1987) *Virology 160*, 271–274.

Bellinger-Kawahara, C. G., Kempner, E., Groth, D. F., Gabizon, R., & Prusiner, S. B. (1988) *Virology 164*, 537–541.

Beyer, T. A., Sadler, J. A., Rearick, J. I., Paulson, J. C., & Hill, R. L. (1981) *Adv. Enzymol. Relat. Areas Mol. Biol. 52*, 23–175.

Bolton, D. C., McKinley, M. P., & Prusiner, S. B. (1982) *Science 218*, 1309–1311.

Bolton, D. C., Meyer, R. K., & Prusiner, S. B. (1985) *J. Virol. 53*, 596–606.

Borchelt, D. R., Scott, M., Taraboulos, A., Stahl, N., & Prusiner, S. B. (1990) *J. Cell Biol. 110*, 743–752.

Bremer, E. G., Hakomori, S., Bowen-Pope, D. F., Raines, E., & Ross, R. (1984) *J. Biol. Chem. 259*, 6818–6825.

Bruce, M. E., & Dickinson, A. G. (1987) *J. Gen. Virol. 68*, 79–89.

Butler, D. A., Scott, M. R. D., Bockman, J. M., Borchelt, D. R., Taraboulos, A., Hsiao, K. K., Kingsbury, D. T., & Prusiner, S. B. (1988) *J. Virol. 62*, 1558–1564.

Carp, R. I., & Callahan, S. M. (1991) *J. Gen. Virol. 72*, 293–298.

Caughey, B., Neary, K., Butler, R., Ernst, D., Perry, L., Cheseboro, B., & Race, R. (1990) *J. Virol. 64*, 1093–1101.

De Cristan, G., Morbidelli, L., Alessandri, G., Ziche, M., Cappa, A. P., & Gullino, P. M. (1990) *J. Cell. Physiol. 144*, 505–510.

Dever, T. E., Costello, C. E., Owens, C. L., Rosenberry, T. L., & Merrick, W. C. (1989) *J. Biol. Chem. 264*, 20518–20525.

Doh-ura, K., Tateishi, J., Sasaki, H., Kitamoto, T., & Sakaki, Y. (1989) *Biochem. Biophys. Res. Commun. 163*, 974–979.

Duguid, J. R., Rohwer, R. G., & Seed, G. (1988) *Proc. Natl. Acad. Sci. U.S.A. 85*, 5738–5742.

Endo, T., Groth, D., Prusiner, S. B., & Kobata, A. (1989) *Biochemistry 28*, 8380–8388.

Feizi, T. (1985) *Nature 314*, 53–57.

Ferguson, M. A. J., Low, M. G., & Cross, G. A. M. (1985) *J. Biol. Chem. 260*, 14547–14555.

Ferguson, M. A. J., Homans, S. W., Dwek, R. A., & Rademacher, T. W. (1988) *Science 239*, 753–759.

Fraser, H., & Dickinson, A. G. (1968) *J. Comp. Pathol. 78*, 301–311.

Gabizon, R., McKinley, M. P., Groth, D., & Prusiner, S. B. (1988) *Proc. Natl. Acad. Sci. U.S.A. 85*, 6617–6621.

Gajdusek, D. C. (1977) *Science 197*, 943–960.

Goldfarb, L., Korczyn, A., Brown, P., Chapman, J., & Gajdusek, D. C. (1990) *Lancet 336*, 637–638.

Goldgaber, D., Goldfarb, L. G., Brown, P., Asher, D. M., Brown, W. T., Lin, S., Teener, J. W., Feinstone, S. M., Rubenstein, R., Kascsak, R. J., Boellaard, J. W., & Gajdusek, D. C. (1989) *Exp. Neurol. 106*, 204–206.

Haraguchi, T., Fisher, S., Olofsson, S., Endo, T., Groth, D., Tarentino, A., Borchelt, D., Teplow, D., Hood, L., Burlingame, A., Lycke, E., Kobata, A., & Prusiner, S. B. (1989) *Arch. Biochem. Biophys. 274*, 1–13.

Hecker, R., Taraboulos, A., Scott, M., Pan, K.-M., Torchia, M., Jendroska, K., DeArmond, S. J., & Prusiner, S. B. (1992) *Genes Dev.* (in press).

Homans, S. W., Ferguson, M. A., Dwek, R. A., Rademacher, T. W., Anand, R., & Williams, A. F. (1988) *Nature (London) 333*, 269–272.

Hope, J., Multhaup, G., Reekie, L. J. D., Kimberlin, R. H., & Beyreuther, K. (1988) *Eur. J. Biochem. 172*, 271–277.

Hsiao, K., & Prusiner, S. B. (1990) *Neurology 40*, 1820–1827.

Hsiao, K., Baker, H. F., Crow, T. J., Poulter, M., Owen, F., Terwilliger, J. D., Westaway, D., Ott, J., & Prusiner, S. B. (1989) *Nature 338*, 342–345.

Hsiao, K. K., Scott, M., Foster, D., Groth, D. F., DeArmond, S. J., & Prusiner, S. B. (1990) *Science 250*, 1587–1590.

Hsiao, K. K., Cass, C., Schellenberg, G., Bird, T., Devine-Gage, E., Wisniewski, H., & Prusiner, S. B. (1991a) *Neurology 41*, 681–684.

Hsiao, K., Meiner, Z., Kahana, E., Cass, C., Kahana, I., Avrahami, D., Scarlato, G., Abramsky, O., Prusiner, S. B., & Gabizon, R. (1991b) *N. Engl. J. Med. 324*, 1091–1097.

Kimberlin, R. H., & Walker, C. A. (1978) *J. Gen. Virol. 39*, 487–496.

Kimberlin, R. H., Cole, S., & Walker, C. A. (1987) *J. Gen. Virol. 68*, 1875–1881.

Laemmli, U. K. (1970) *Nature (London) 235*, 383–386.

Low, M. G., & Saltiel, A. R. (1988) *Science 239*, 268–275.

Masters, C. L., Gajdusek, D. C., & Gibbs, C. J., Jr. (1981) *Brain 104*, 559–588.

Mayor, S., Menon, A. K., Cross, G. A. M., Ferguson, M. A. J., Dwek, R. A., & Rademacher, T. W. (1990) *J. Biol. Chem. 265*, 6164–6173.

McKinley, M. P., Bolton, D. C., & Prusiner, S. B. (1983) *Cell 35*, 57–62.

McKinley, M. P., Meyer, R. K., Kenaga, L., Rahbar, F., Cotter, R., Serban, A., & Prusiner, S. B. (1991) *J. Virol. 65*, 1340–1351.

Meyer, R. K., McKinley, M. P., Bowman, K. A., Braunfeld, M. B., Barry, R. A., & Prusiner, S. B. (1986) *Proc. Natl. Acad. Sci. U.S.A. 83*, 2310–2314.

Meyer, N., Rosenbaum, V., Schmidt, B., Gilles, K., Mirenda, C., Groth, D., Prusiner, S. B., & Riesner, D. (1991) *J. Gen. Virol. 72*, 37–49.

Nojiri, H., Stroud, M., & Hakomori, S. (1991) *J. Biol. Chem. 266*, 4531–4537.

Oesch, B., Groth, D. F., Prusiner, S. B., & Weissmann, C. (1988) *Ciba Found. Symp. 135*, 209–223.

Offner, H., Thieme, T., & Vandenbark, A. A. (1987) *J. Immunol. 139*, 3295–3305.

Owen, F., Poulter, M., Lofthouse, R., Collinge, J., Crow, T. J., Risby, D., Baker, H. F., Ridley, R. M., Hsiao, K., &

Prusiner, S. B. (1989) *Lancet 1*, 51-52.
Paulson, J. C., & Colley, K. J. (1989) *J. Biol. Chem. 264*, 17615-17618.
Prusiner, S. B. (1982) *Science 216*, 136-244.
Prusiner, S. B. (1991) *Science 252*, 1515-1522.
Prusiner, S. B. (1987) *N. Engl. J. Med. 317*, 1571-1581.
Prusiner, S. B., Scott, M., Foster, D., Pan, K.-M., Groth, D., Mirenda, C., Torchia, M., Yang, S.-Y., Serban, D., Carlson, G. A., Hoppe, P. C., Westaway, D., & DeArmond, S. J. (1990) *Cell 63*, 673-686.
Rademacher, T. W., Parekh, R. B., & Dwek, R. A. (1988) *Annu. Rev. Biochem. 57*, 785-838.
Roberts, W. L., Santikarn, S., Reinhold, V. N., & Rosenberry, T. L. (1988) *J. Biol. Chem. 263*, 18776-18784.
Romero, G., Luttrell, L., Rogol, A., Zeller, K., Hewlett, E., & Larner, J. (1988) *Science 240*, 509-511.
Rosen, S. D., Chi, S. I., True, D. D., Singer, M. S., & Yednock, T. A. (1989) *J. Immunol. 142*, 1895-1902.
Safar, J., Wang, W., Padgett, M. P., Ceroni, M., Piccardo, P., Zopf, D., Gajdusek, D. C., & Gibbs, C. J., Jr. (1990) *Proc. Natl. Acad. Sci. U.S.A. 87*, 6373-6377.
Samlowski, W. E., Spangrude, G. J., & Daynes, R. A. (1984) *Cell. Immunol. 88*, 309-322.
Schenkman, S., Jiang, M.-S., Hart, G. W., & Nussenzweig, V. (1991) *Cell 65*, 1117-1125.
Schmitz, B., Klein, R. A., Duncan, I. A., Egge, H., Gunawan, J., Peter-Katalinic, J., Dabrowski, U., & Dabrowski, J. (1987) *Biochem. Biophys. Res. Commun. 146*, 1055-1063.
Schneider, P., Ferguson, M. A. J., McConville, M. J., Mehlert, A., Homans, S. W., & Bordier, C. (1990) *J. Biol. Chem. 265*, 16955-16964.
Scott, M., Foster, D., Mirenda, C., Serban, D., Coufal, F., Walchli, M., Torchia, M., Groth, D., Carlson, G., DeArmond, S. J., Westaway, D., & Prusiner, S. B. (1989) *Cell 59*, 847-857.
Singh, N., Singleton, D., & Tartakoff, A. M. (1991) *Mol. Cell. Biol. 11*, 2362-2374.
Stahl, N., & Prusiner, S. B. (1991) *FASEB J. 5*, 2799-2807.
Stahl, N., Borchelt, D. R., Hsiao, K., & Prusiner, S. B. (1987) *Cell 51*, 229-240.
Stahl, N., Baldwin, M. A., Burlingame, A. L., & Prusiner, S. B. (1990a) *Biochemistry 29*, 8879-8884.
Stahl, N., Borchelt, D. R., & Prusiner, S. B. (1990b) *Biochemistry 29*, 5405-5412.
Stahl, N., Borchelt, D. R., & Prusiner, S. B. (1990c) in *Molecular and Cell Biology of Membrane Proteins* (Turner, A. J., Ed.) pp 189-216, Ellis Horwood Limited, London.
Sulkowski, E. (1989) *BioEssays 10*, 170-175.
Taguchi, R., Asahi, Y., & Ikezawa, H. (1980) *Biochim. Biophys. Acta 619*, 48-57.
Taraboulos, A., Rogers, M., Borchelt, D. R., McKinley, M. P., Scott, M., Serban, D., & Prusiner, S. B. (1990) *Proc. Natl. Acad. Sci. U.S.A. 87*, 8262-8266.
Tartakoff, A. M., & Vassalli, P. (1983) *J. Cell Biol. 97*, 1243-1248.
Tsuji, S., Arita, M., & Nagai, Y. (1983) *J. Biochem. 94*, 303-306.
Turk, E., Teplow, S. B., Hood, L. E., & Prusiner, S. B. (1988) *Eur. J. Biochem. 176*, 21-30.
Wilesmith, J. W., Wells, G. A. H., Cranwell, M. P., & Ryan, J. B. M. (1988) *Vet. Rec. 123*, 638-634.
Zingales, B., Carniol, C., de Lederkremer, R. M., & Colli, W. (1987) *Mol. Biochem. Parasitol. 26*, 135-144.

Biophysical Characterization of a Transit Peptide Directing Chloroplast Protein Import†

Steven M. Theg* and F. Jon Geske
Department of Botany, University of California, Davis, California 95616
Received October 11, 1991; Revised Manuscript Received March 19, 1992

ABSTRACT: We have investigated the biophysical properties of a 35 amino acid peptide representing the entire length of a chloroplastic targeting sequence. The peptide, termed γ-tp, corresponds in sequence to the transit peptide of the γ subunit of the chloroplast ATP synthase from *Chlamydomonas reinhardtii*. We found that γ-tp blocks the import of the small subunit of ribulose-1,5-bisphosphate carboxylase/oxygenase into isolated pea chloroplasts ($K_I \approx 5$ μM), suggesting that it interacts with higher plant plastids in a physiological manner. We also found the γ-tp to have a high affinity for nonpolar environments, but not to cause a general disruption of membrane integrity. Hydrophobic moment analysis suggests that the γ-tp can adopt an amphipathic β structure. However, circular dichroism measurements indicate that the peptide is largely a random coil, in both the presence and absence of sodium laurylsulfate micelles. In the absence of a recognizable secondary structural targeting motif, we asked whether the presence of a transit peptide on a chloroplast protein increases the protein's overall affinity for nonpolar environments. Phase-partition experiments with Triton X-114 suggest that this is not the case. These results are discussed in relation to the mechanism of protein targeting to chloroplasts.

Chloroplasts and mitochondria are unique among organelles in that they are capable of a certain amount of semiautonomous protein synthesis. Nonetheless, most of their complement of proteins is encoded in the nucleus, synthesized on cytoplasmic ribosomes, and taken up posttranslationally by the organelles. Proteins destined for these organelles are synthesized as high molecular weight precursors and contain an amino-terminal extension of amino acids termed a transit

† This work was supported in part by National Science Foundation Grant DCB88-17373 to S.M.T.
* Address correspondence to this author.

0006-2960/92/0431-5053$03.00/0